Electronic Supporting Information (ESI)

for

Synthesis, Structure, and Electrochemical Properties of [LNi(R$_f$)(C$_4$F$_8$)]$^-$ and [LNi(R$_f$)$_3$]$^-$ Complexes

Scott T. Shreiber,[#a] Fatema Amin,[#a] Sascha A. Schäfer,[b] Roger E. Cramer,[c] Axel Klein [b]* and David A. Vicic[a]*

[a] Department of Chemistry, Lehigh University, 6 E Packer Ave., Bethlehem, PA 18015, USA. Email: sts217@lehigh.edu; ORCID: 0000-0002-4224-7461 (S.T.S); E-mail: fab319@lehigh.edu; ORCID: 0000-0002-8420-1912 (F.A.).

[b] University of Cologne, Faculty of Mathematics and Natural Sciences, Department of Chemistry, Institute for Inorganic Chemistry, Greinstrasse 6, 50939 Koeln, Germany. E-mail: sascha.schaefer@uni-koeln.de; ORCID: 0000-0003-0093-9619 (S.A.S.).

[c] Department of Chemistry, University of Hawaii, 2545 McCarthy Mall, Honolulu, HI, 96822, USA. E-mail: rcramer@hawaii.edu ORCID: 0000-0002-3934-3401 (R.E.C.).

[#]These authors contributed equally to this work.

* Corresponding authors: E-mail: axel.klein@uni-koeln.de, ORCID: 0000-0003-0093-9619; Tel.: +49-221-470-4006 (A.K.). E-mail: vicic@lehigh.edu; fax, 1-610-758-6536, ORCID: 0000-0002-4990-0355 (D.A.V.)

Contents:

Fig. S23 400 MHz ^{1}H NMR and 470.6 MHz ^{19}F NMR spectra of **9** and **9'** in CD$_3$CN.

Fig. S24 Cyclic voltammograms of **1**, **2**, and **4** in MeCN/*n*-Bu$_4$NPF$_6$.

Fig. S25 Cyclic voltammograms of **5** and **6** in MeCN/*n*-Bu$_4$NPF$_6$.

Fig. S26 Cyclic voltammograms of [NEt$_4$][(IMes)Ni(CF$_3$)$_3$] (**6**) and [NEt$_4$][(2,4-F$_2$Ph-NHC)Ni(CF$_3$)$_3$] (**7**).

Fig. S27 Cyclic voltammograms of [NEt$_4$][(2,4,6-F$_3$Ph-NHC)Ni(CF$_3$)$_3$] (**8**) and [NEt$_4$][(3,4,5-F$_3$Ph-NHC)Ni(CF$_3$)$_3$] (**9**).

Table S1. Selected structure solution and refinement data for nickel complexes **6'**, **7**, **9**, and **9'**.

Table S2 Selected structure solution and refinement data for [PNP]$_2$[Ni$_2$(CF$_3$)$_4$(μ-F)$_2$]·2THF.


Supporting Figures
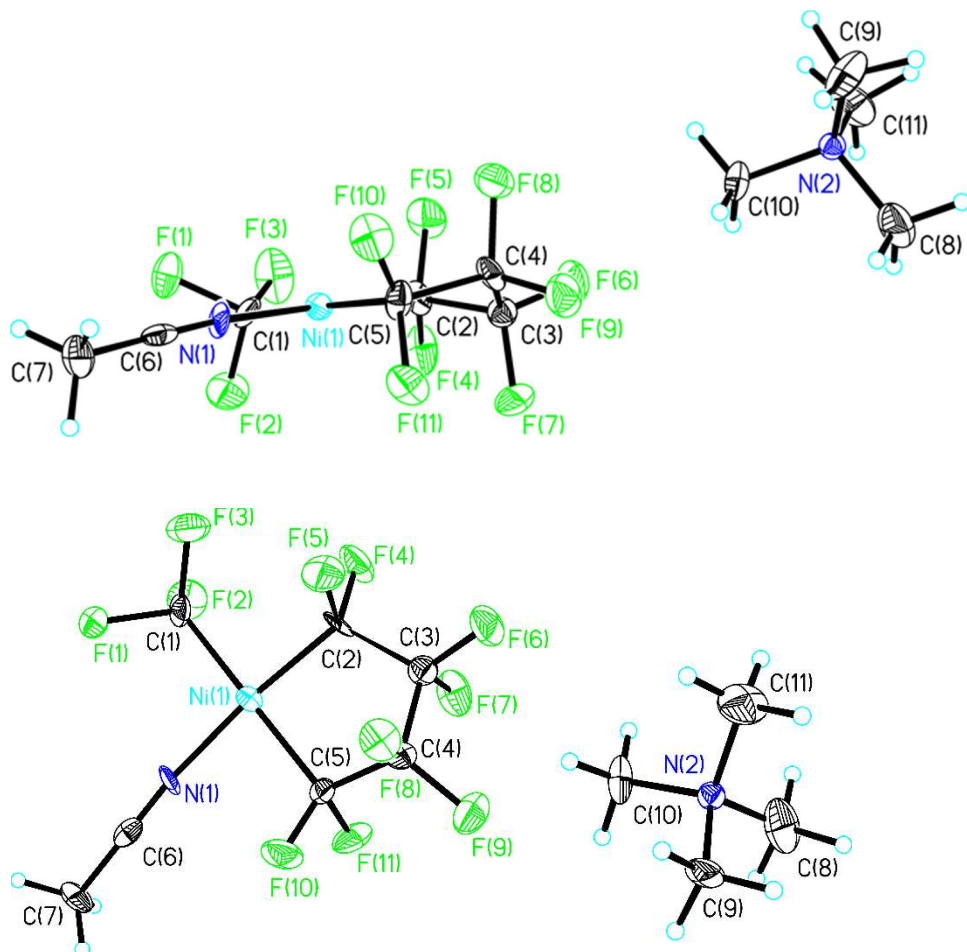
**Fig. S1** Views on the crystals structure of **2**.
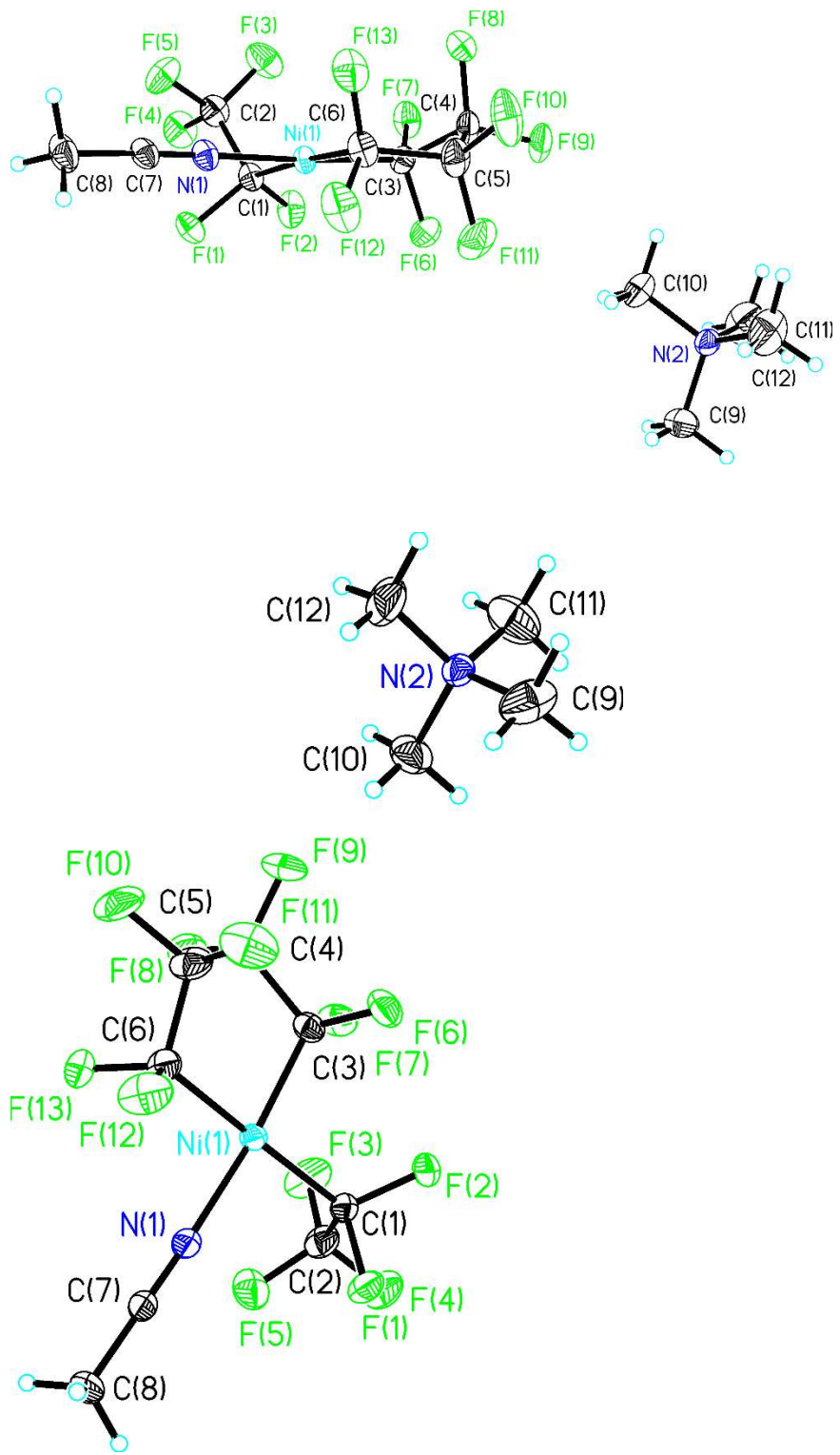
**Fig. S2.** Views on the crystal structure of **3**.
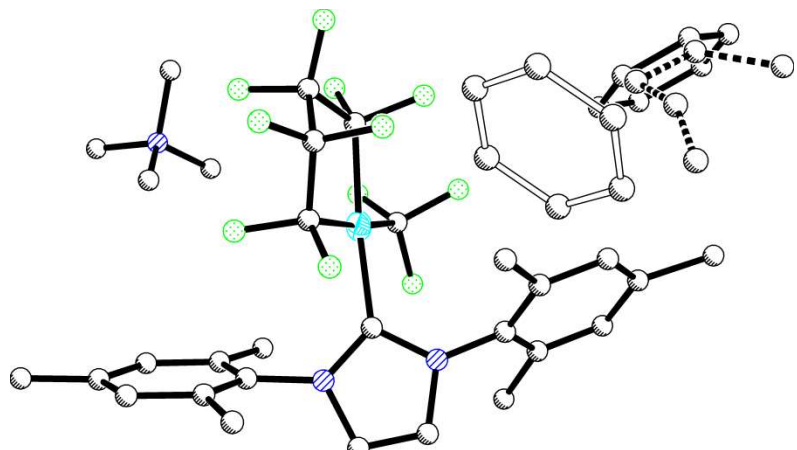
Fig. S3 Preliminary X-ray data for compound **4·pentane·2benzene**. Only a poorly refined data set with two co-crystallized benzene molecules and one co-crystallized pentane could been obtained for compound **4**. The preliminary structure shown here is only provided as additional support of the connectivity assignment in the text.
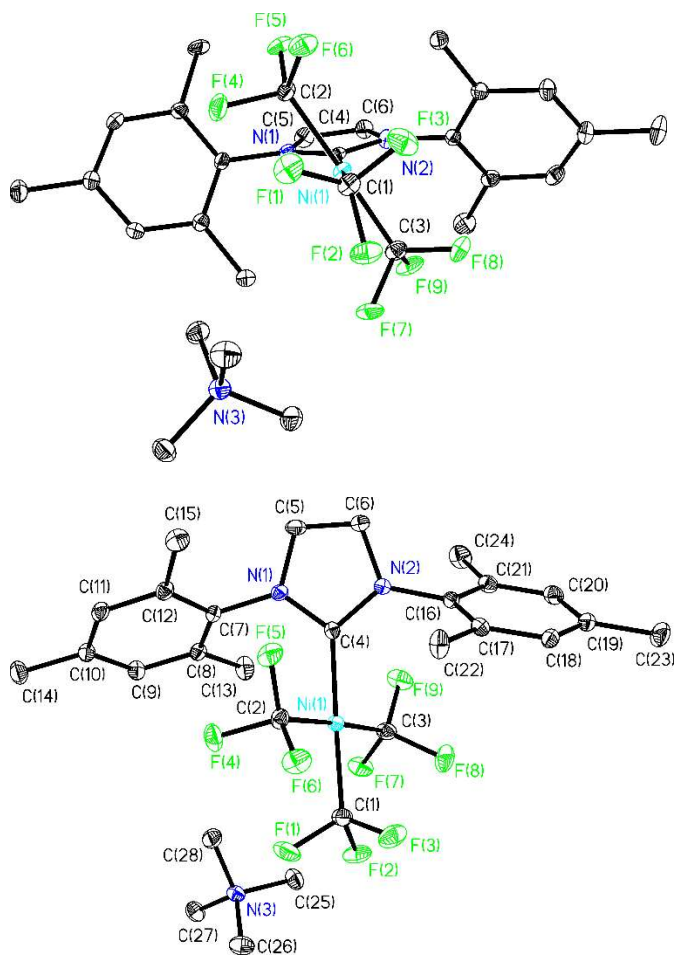

**Fig. S4.** Views on the crystal structure of **6**.
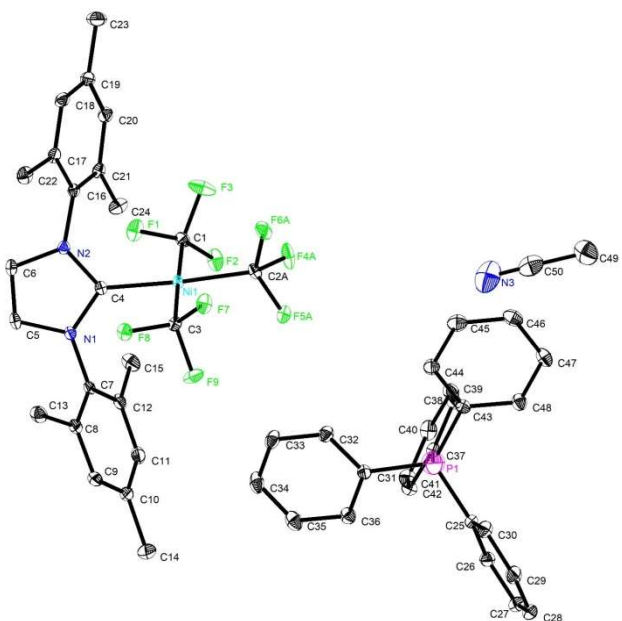
Fig. S5 ORTEP diagram of **6′·MeCN** = [PPh₄][Ni(IMes)(CF₃)₃]·MeCN. Ellipsoids shown at the 40% level. Hydrogen atoms as well as a positional disorder of C2 are omitted for clarity.
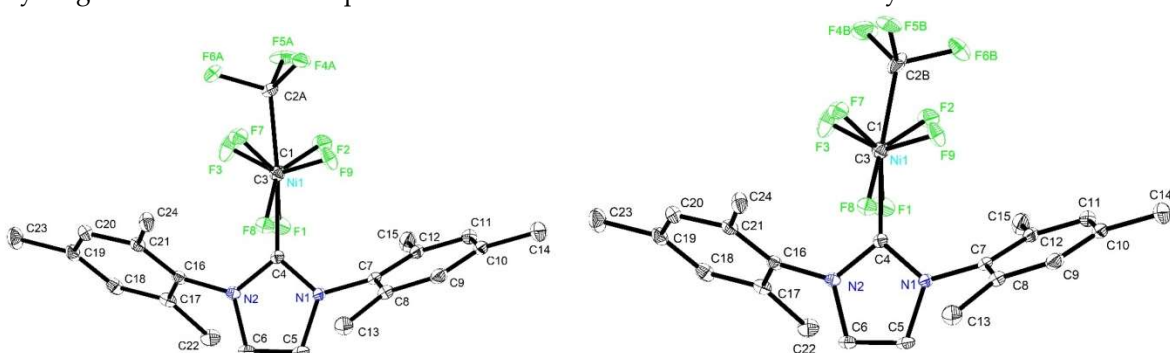
**Fig. S6** ORTEP diagrams of **6′·MeCN** = [PPh₄][Ni(IMes)(CF₃)₃]·MeCN. Ellipsoids shown at the 40% level. Hydrogen atoms, co-crystallized solvent and counter cations are omitted for clarity. The left structure shows the major species with a chemical occupancy of 83.2% and a C4–Ni1–C2A bond angle of 174.23°. The right structure is the minor species with a chemical occupancy of 16.8% and C4–Ni1–C2B bond angle of 169.0°.
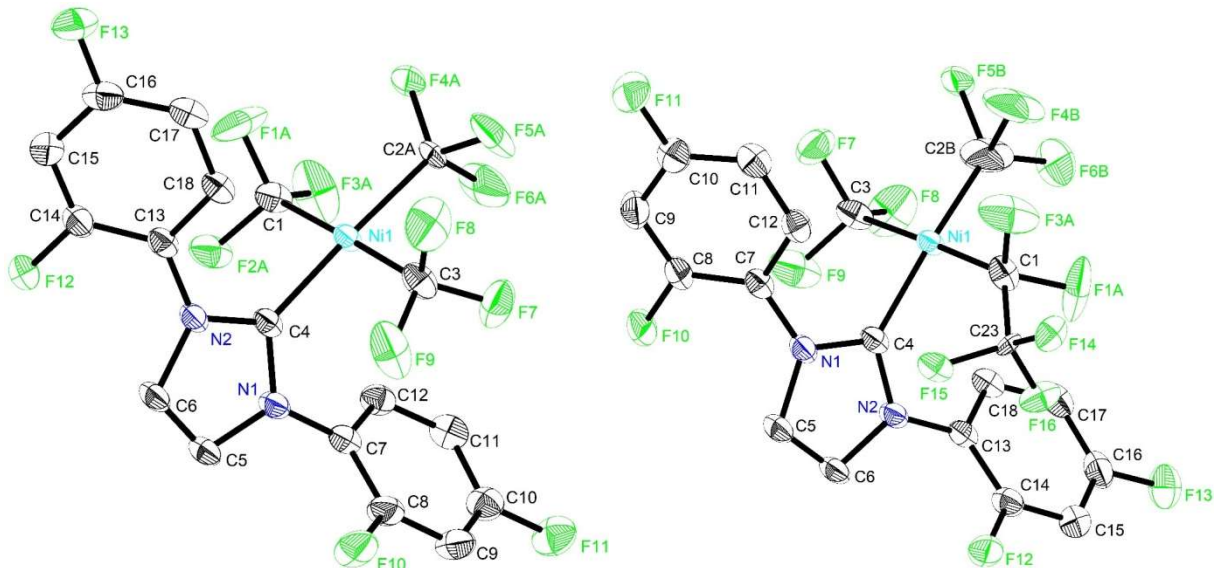
Fig. S7 ORTEP diagrams of **7** (left) and **7'** (right). Ellipsoids shown at the 40% level. Hydrogen atoms and counter cations are omitted for clarity. Both structures were generated from the same XRD measurement. Compound **7'** is present with a chemical occupancy of 12.5%. The right diagram additionally shows the split position of carbon C2A/C2B, with the respective bond angles for C2A–Ni1–C4 176.33(15)° and C2B–Ni1–C4 173.8(9)°. C2B shows a chemical occupancy of 26.3(6)%. Besides the shown partial placement of a C_2F_5 along C1 a rotational disorder of the CF_3 function centered on C1 is observed with a chemical occupancy of 22.9(6)%, and is omitted from the diagrams for clarity.
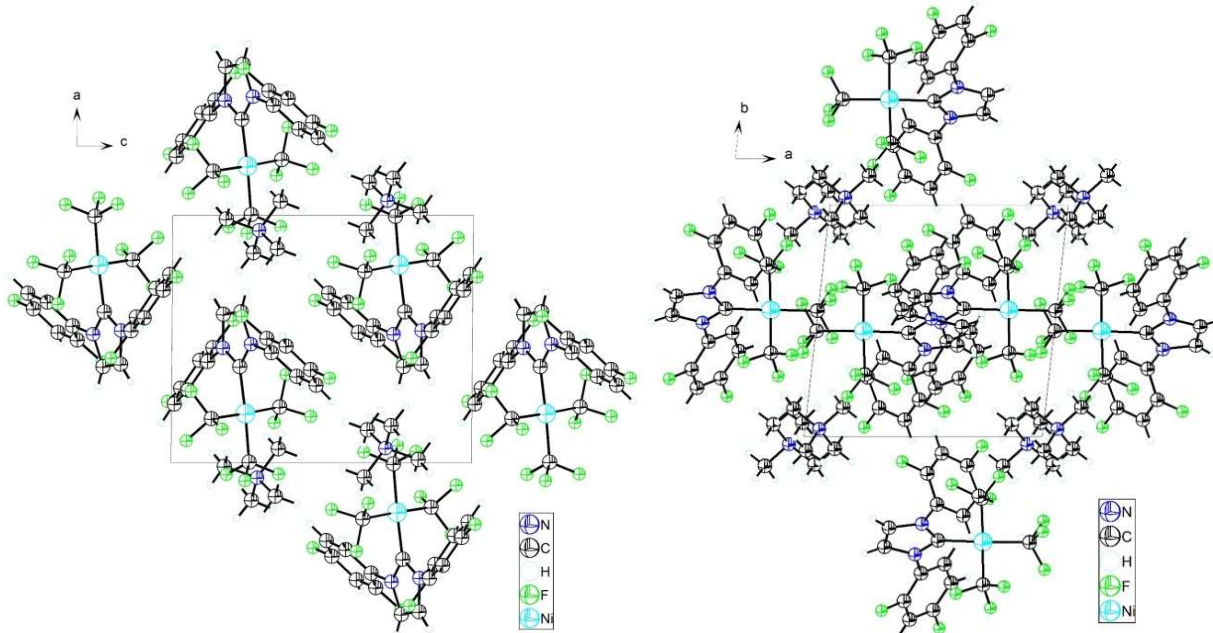

Fig. S8 View on the crystal structure of **7**, shown along the crystallographic b and c axis.
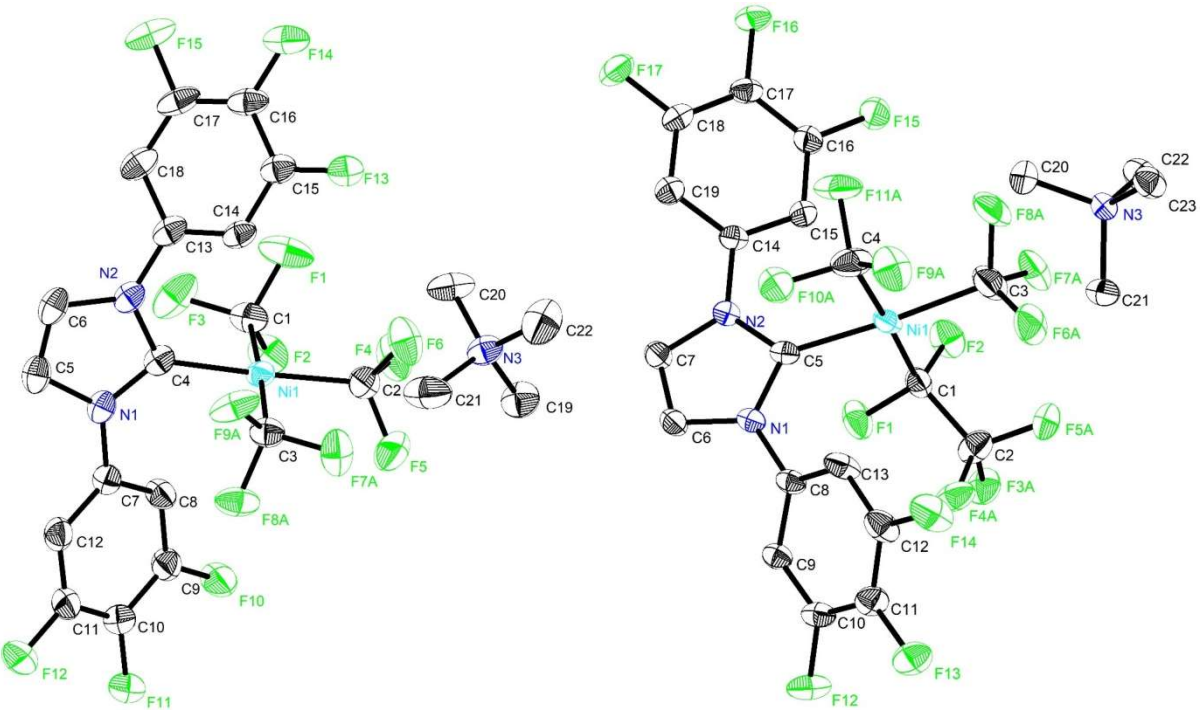
Fig. S9 ORTEP diagrams of **9** (left) and **9'** (right). Ellipsoids shown at the 40% level. Hydrogen atoms are omitted for clarity. In the structure of **9'** 2 equivalents of THF are omitted for clarity. In contrast to compound **7 / 7'** these two compounds crystallized separately and were measured independently. Both structures show rotational disorder of CF$_3$ functions. Compound **9'** additionally shows a C4–CF$_3$/–C$_2$F$_5$ disorder on C4, where one F atom is exchanged for an additional CF$_3$ function with a chemical occupancy of 20%.
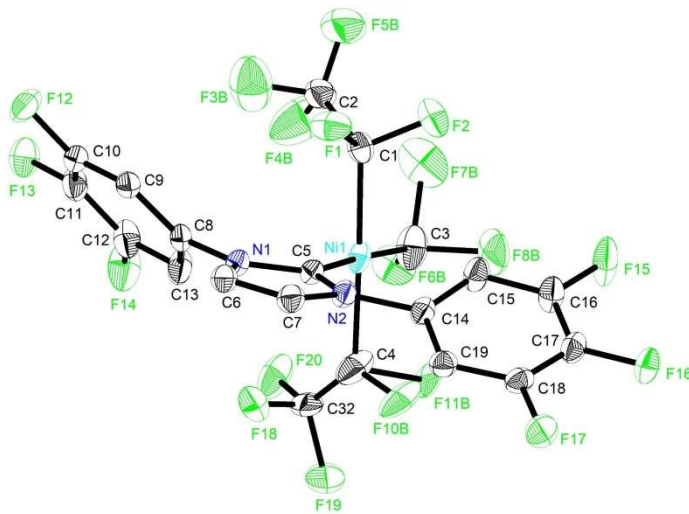

Fig. S10 ORTEP diagram of **9''**, the minor species (20%) found in a crystal of **9'**, showing both the rotational and chemical disorder. Ellipsoids shown at the 40% level. Hydrogen atoms, co-crystallized THF and counter cation are omitted for clarity.
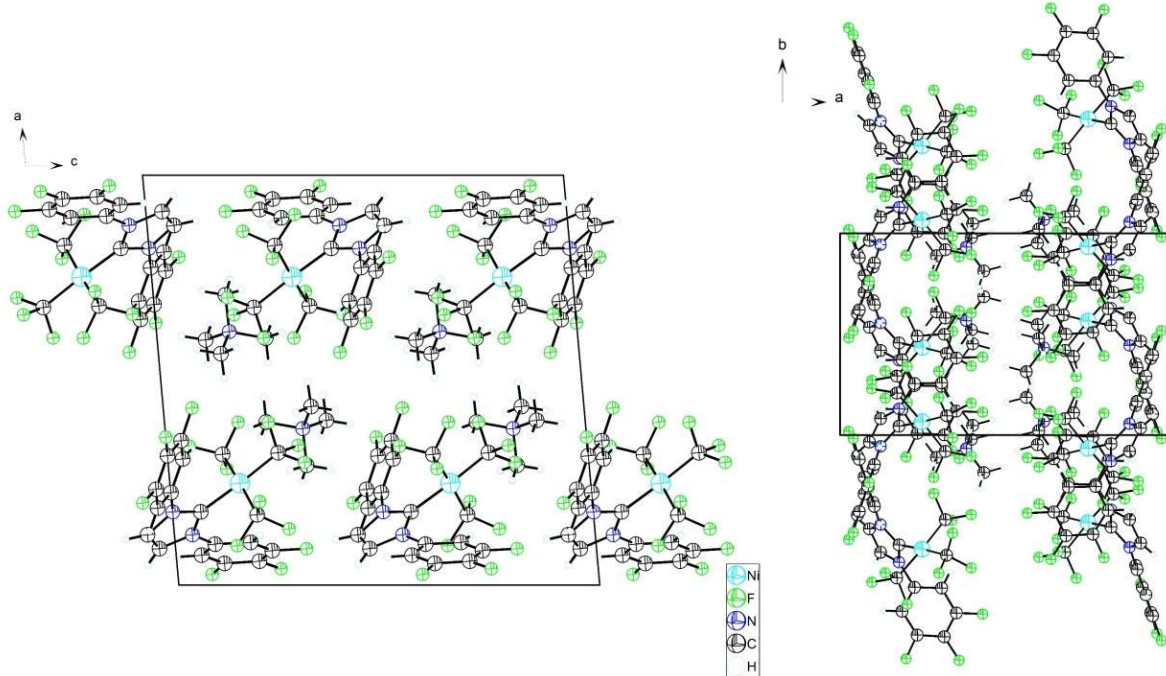
Fig. S11 Views on the crystal structure of **9** along the crystallographic *b* and *c* axis.
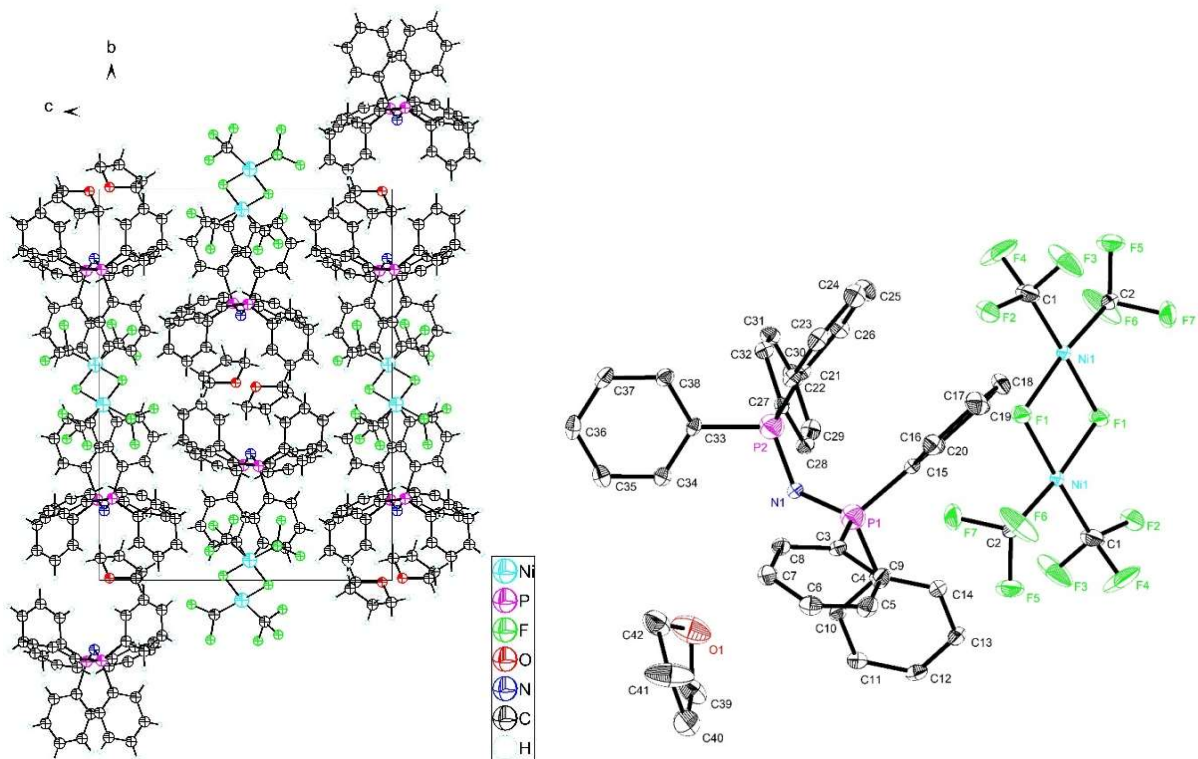

Fig. S12 View on the crystal structure of [PNP]₂[Ni₂(CF₃)₄(μ-F)₂]·2THF along the crystallographic *a* axis (right) and ORTEP diagram of [Ni₂(CF₃)₄(μ-F)₂] (right). Ellipsoids shown at the 40% level. Hydrogen atoms, as well as one molecule each of [PNP]⁺ and THF molecules are omitted for clarity.
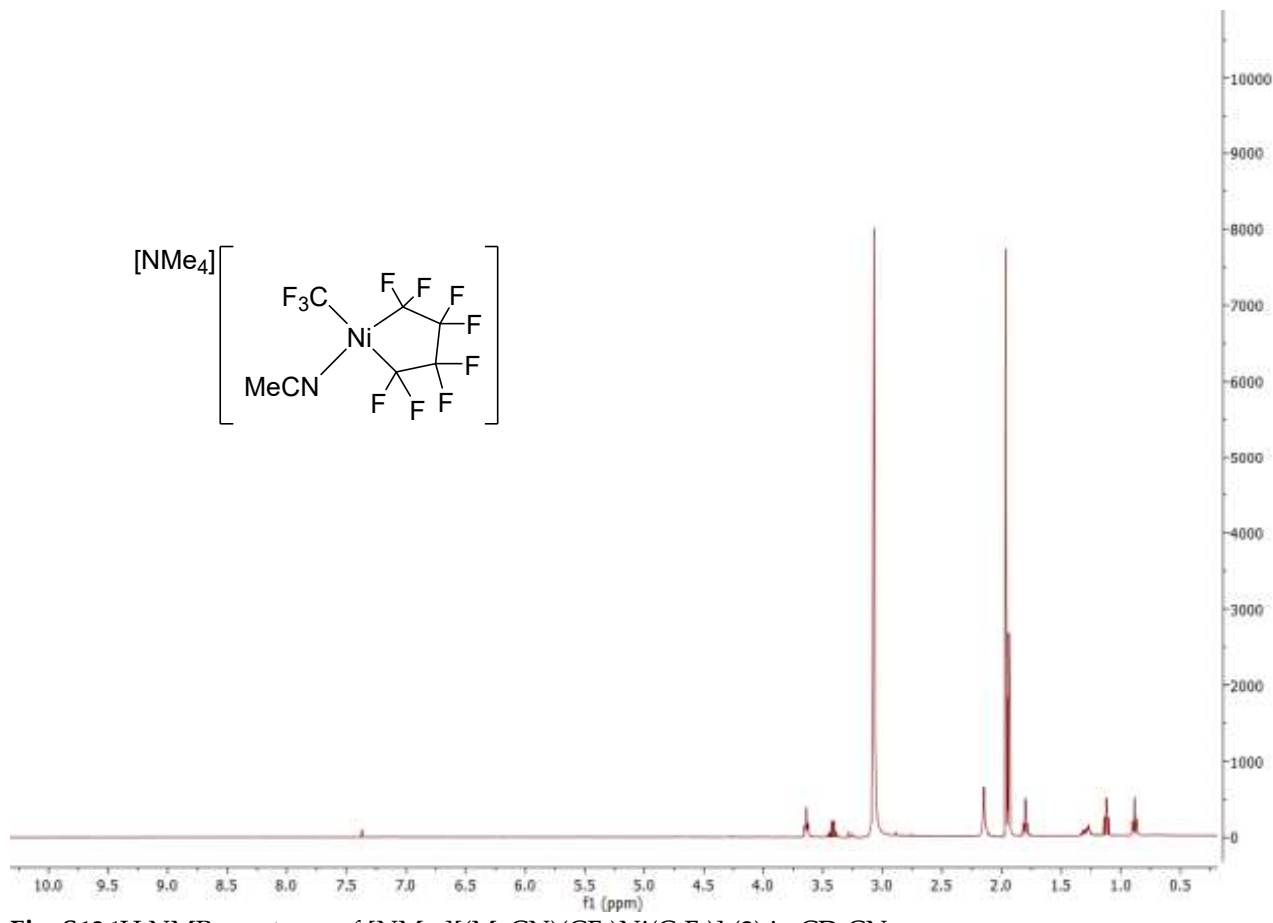
**Fig. S13** ^{1}H NMR spectrum of [NMe$_4$][(MeCN)(CF$_3$)Ni(C$_4$F$_8$)] (**2**) in CD$_3$CN
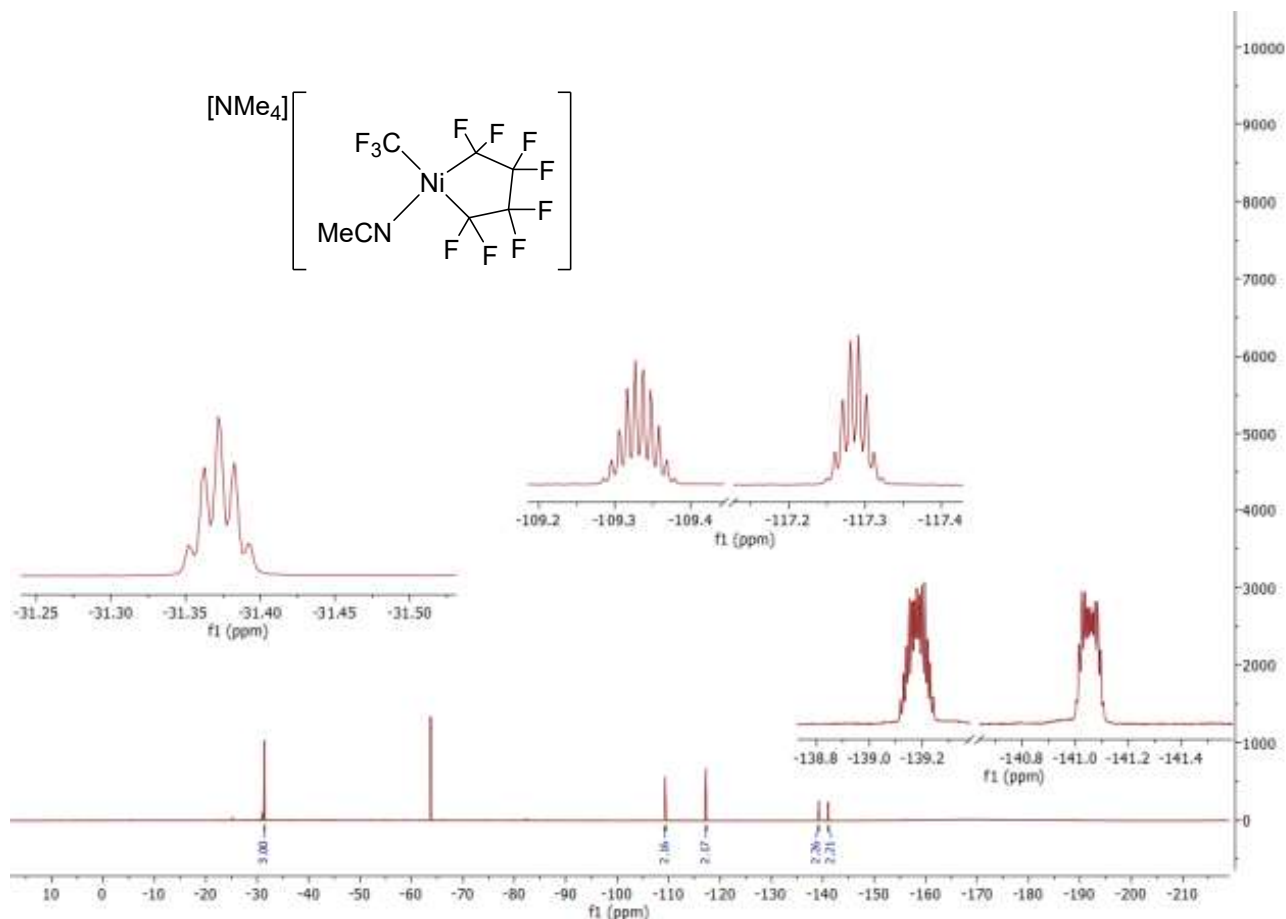
Fig. S14 376 MHz ^{19}F NMR spectrum of **2** in CD$_3$CN.
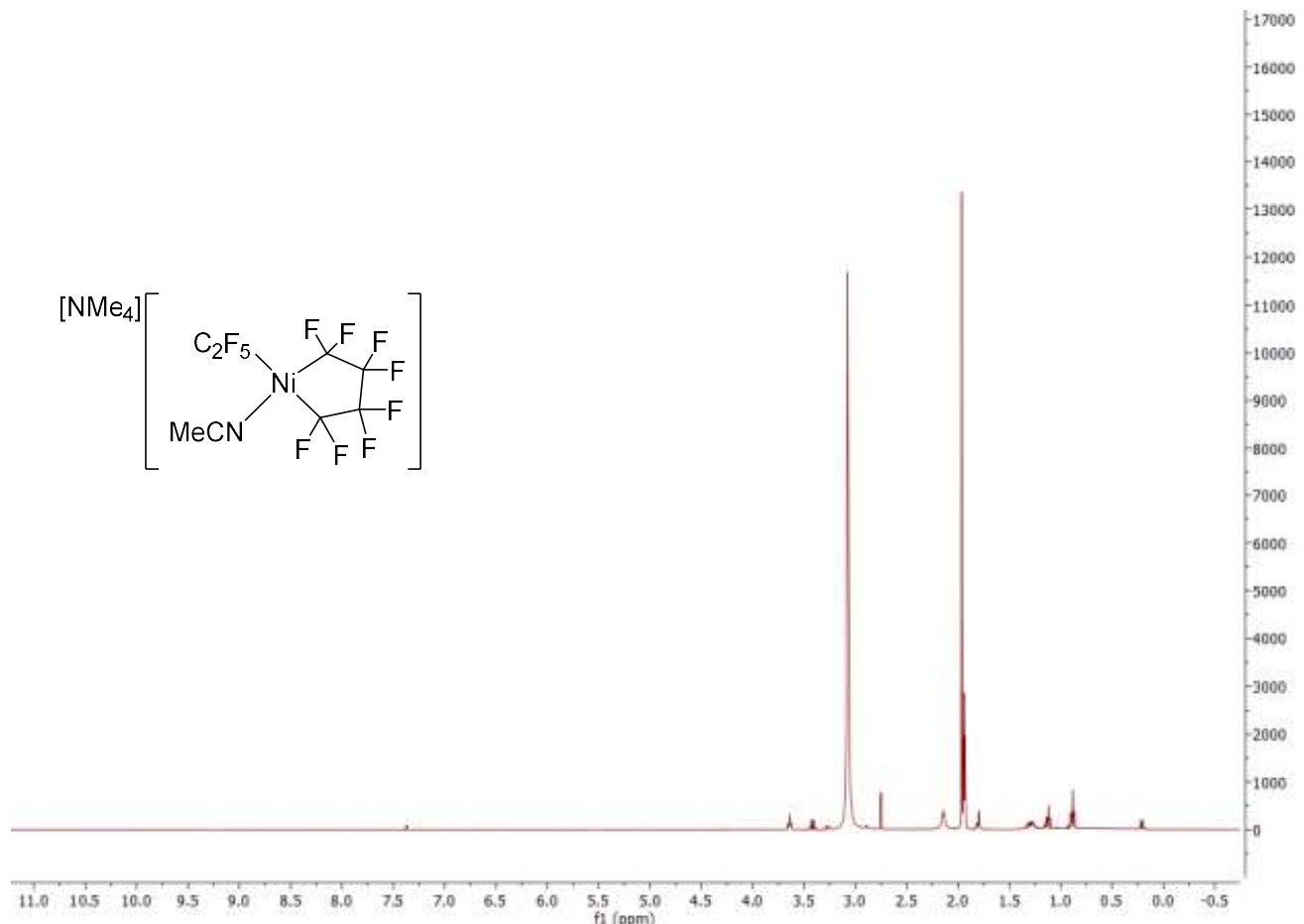
Fig. S15 ^{1}H NMR of [NMe$_4$][(MeCN)(C$_2$F$_5$)Ni(C$_4$F$_8$)] (**3**) in CD$_3$CN.

**Fig. S16** 376 MHz ^{19}F NMR spectra of **3** in CD$_3$CN.
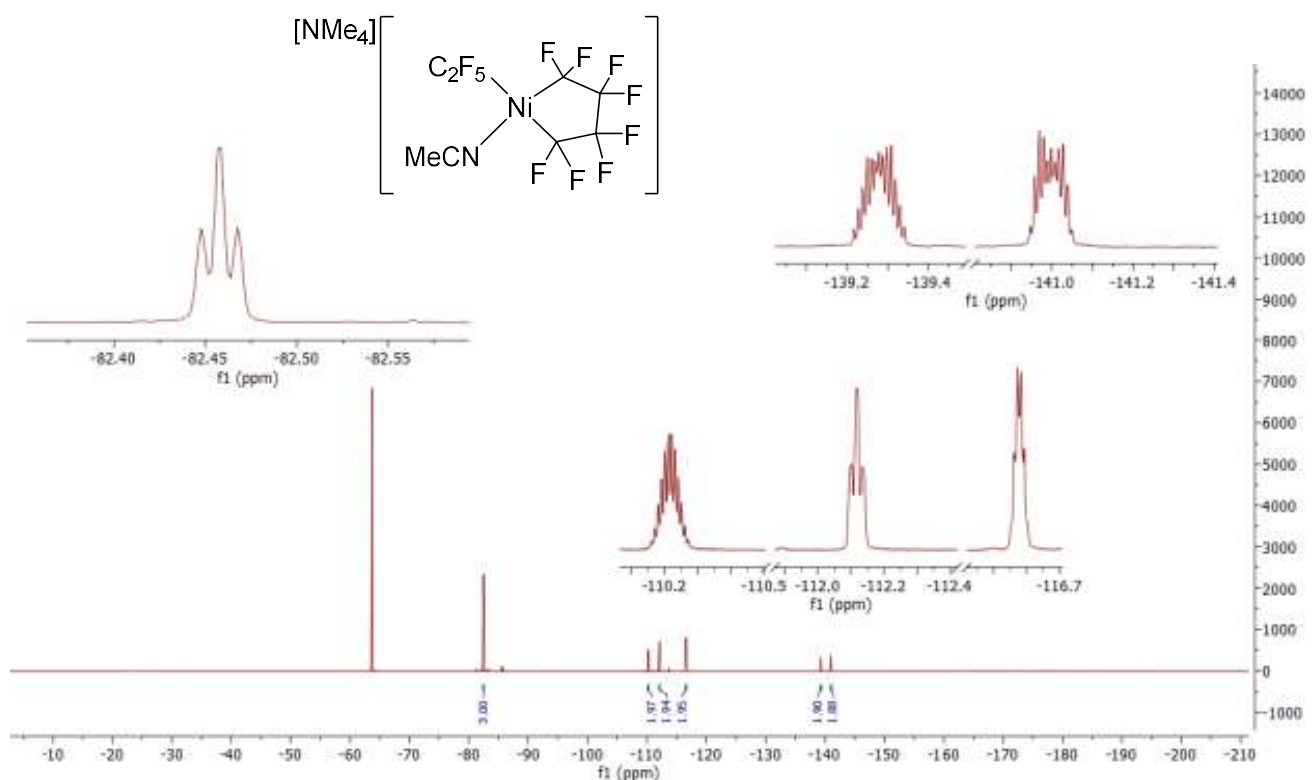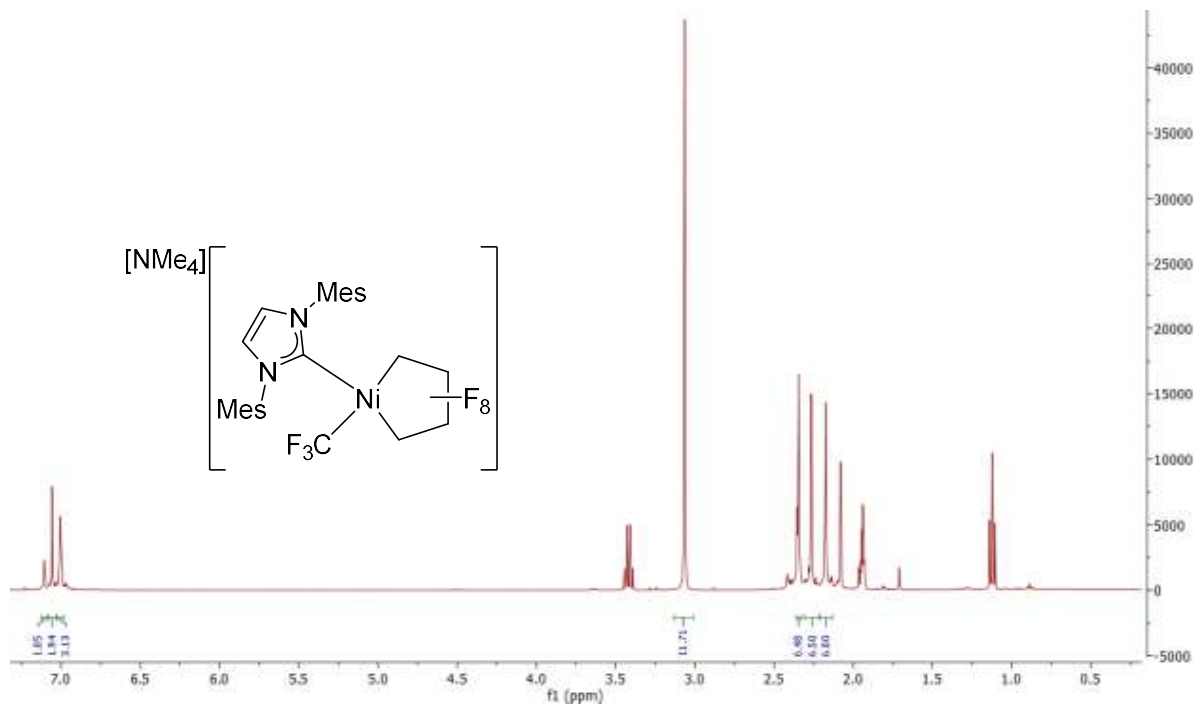
Fig. S17 400 MHz ¹H NMR spectrum of **4** in CD₃CN.
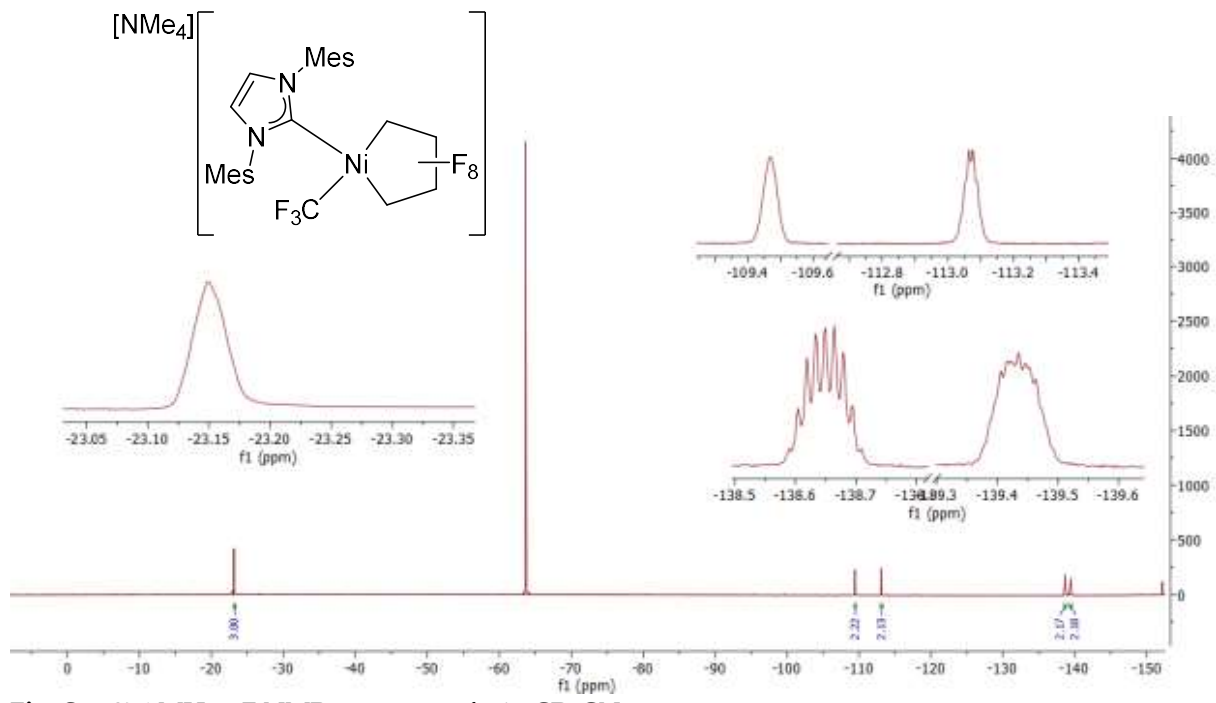
Fig. S18 376 MHz ^{19}F NMR spectrum of **4** in CD$_3$CN.
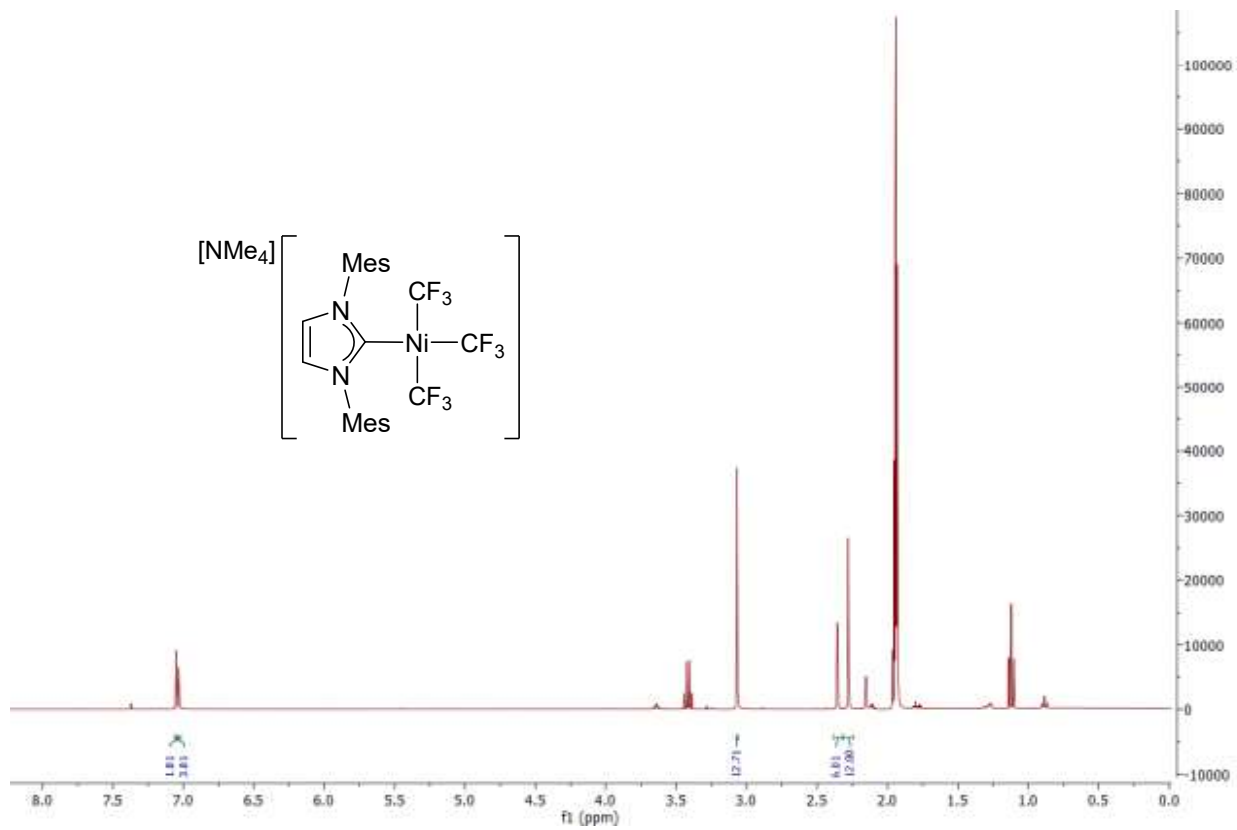
Fig. S19 400 MHz ^{1}H NMR spectrum of **6** in CD$_3$CN.
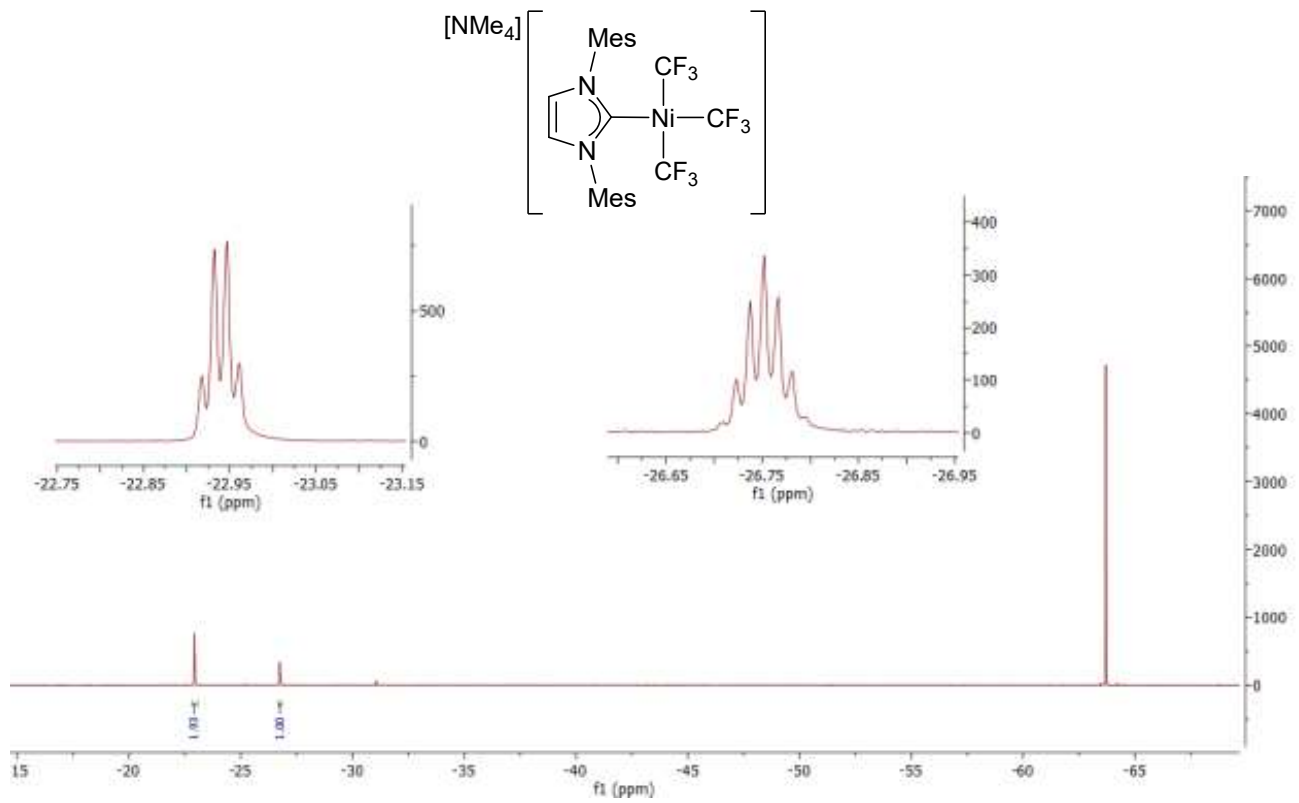
Fig. S20 376 MHz ^{19}F NMR spectrum of **6** in CD$_3$CN.

Fig. S21A 400 MHz ^{1}H NMR and 470.6 MHz ^{19}F NMR spectra of **7** and **7′** in CD$_3$CN.
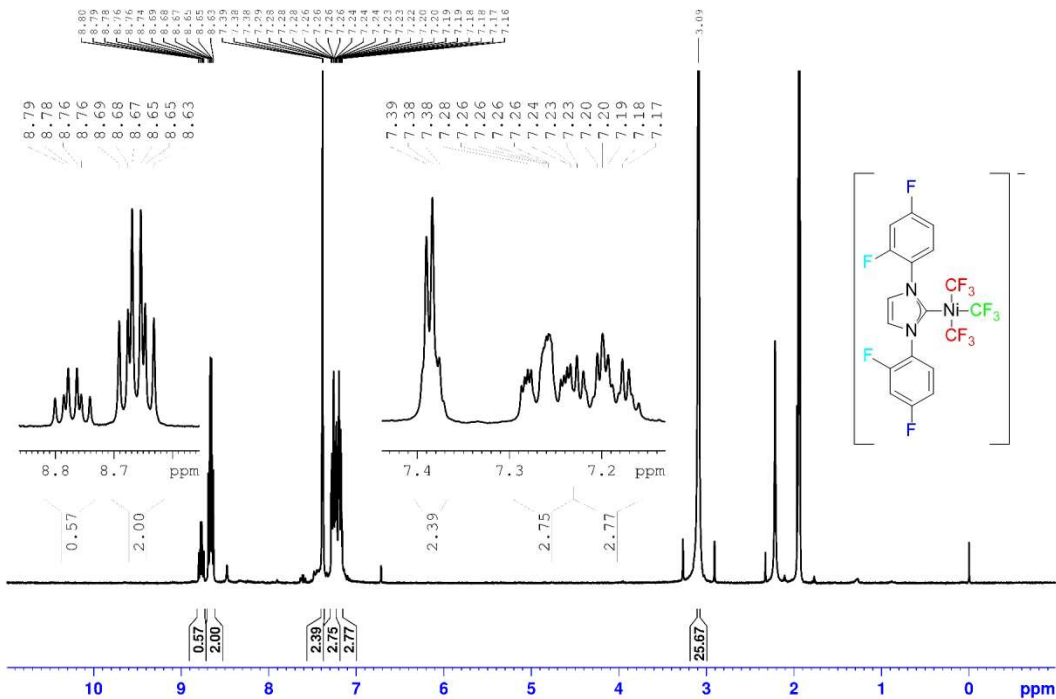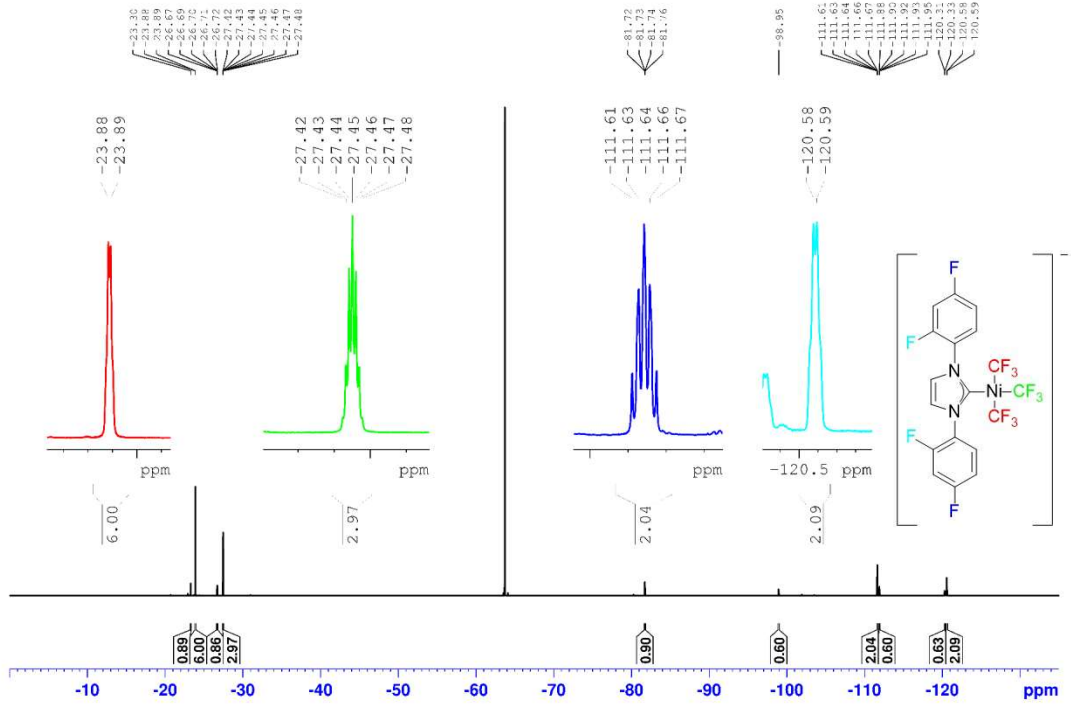
Fig. S21B 400 MHz ^{1}H NMR and 470.6 MHz ^{19}F NMR spectra of **7** and **7′** in CD$_3$CN.
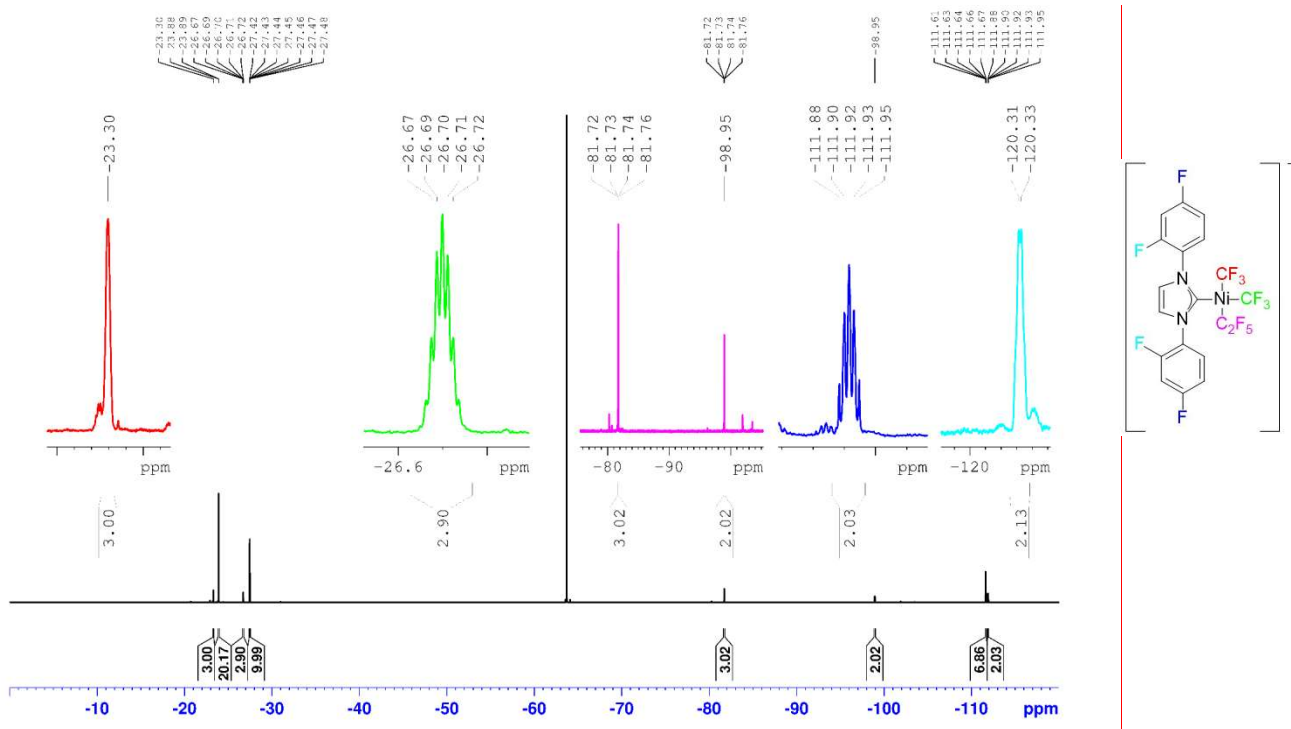
Fig. S21C 400 MHz ^{1}H NMR and 470.6 MHz ^{19}F NMR spectra of **7** and **7′** in CD$_3$CN.
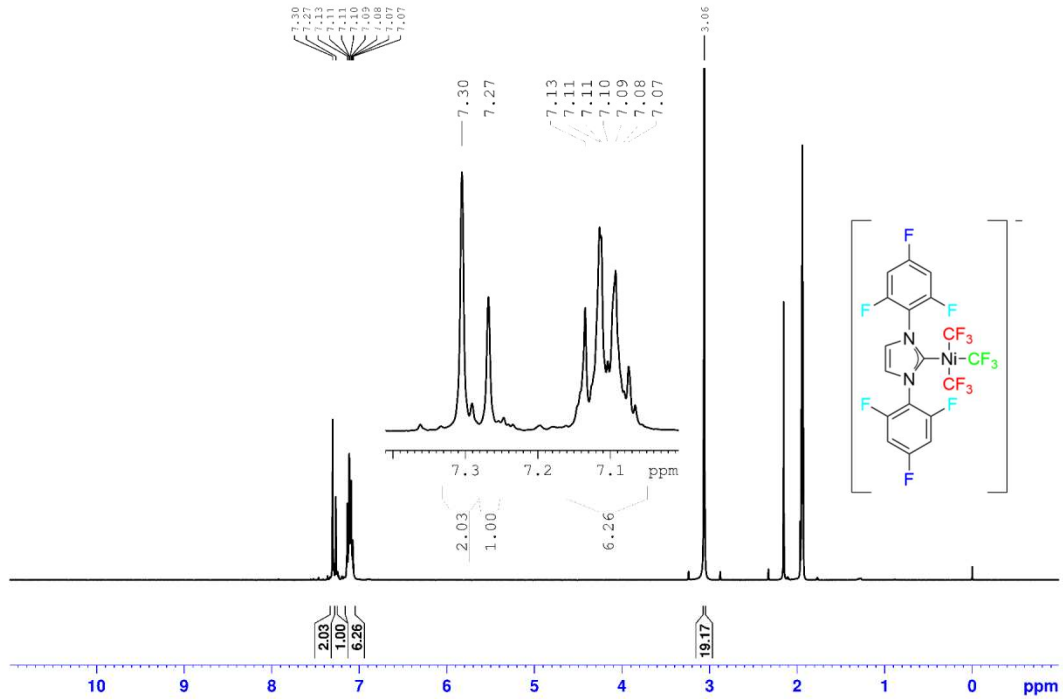
Fig. S22A 400 MHz ¹H NMR and 470.6 MHz ¹⁹F NMR spectra of **8** and **8′** in CD₃CN.
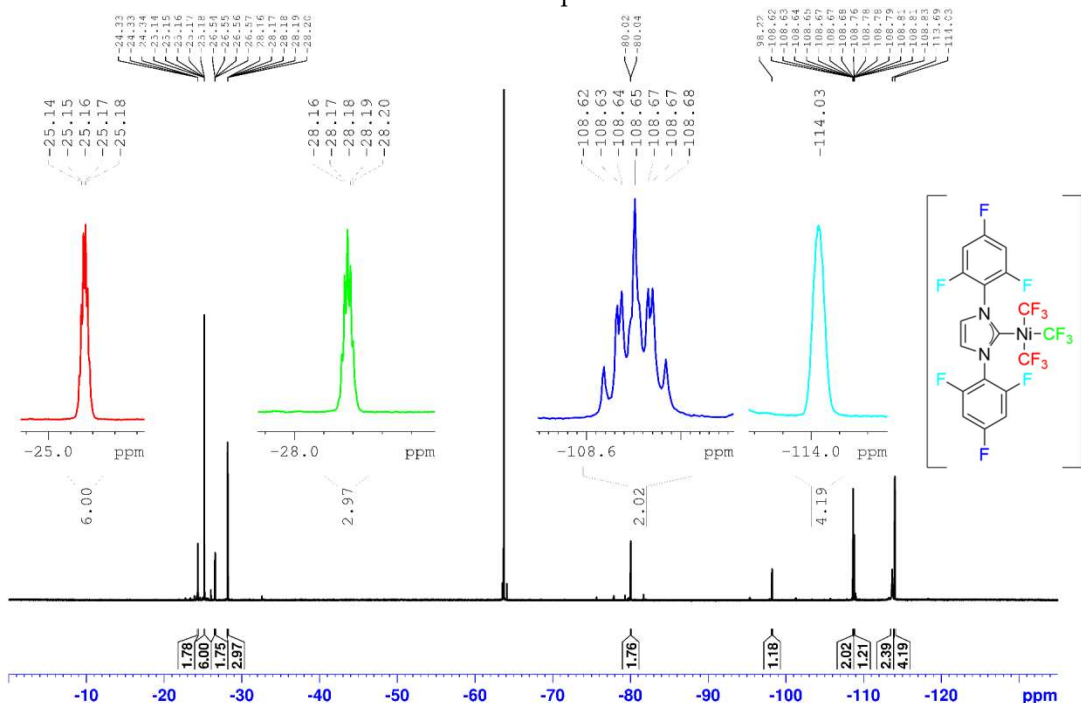
Fig. S22B 400 MHz ¹H NMR and 470.6 MHz ¹⁹F NMR spectra of **8** and **8′** in CD₃CN.
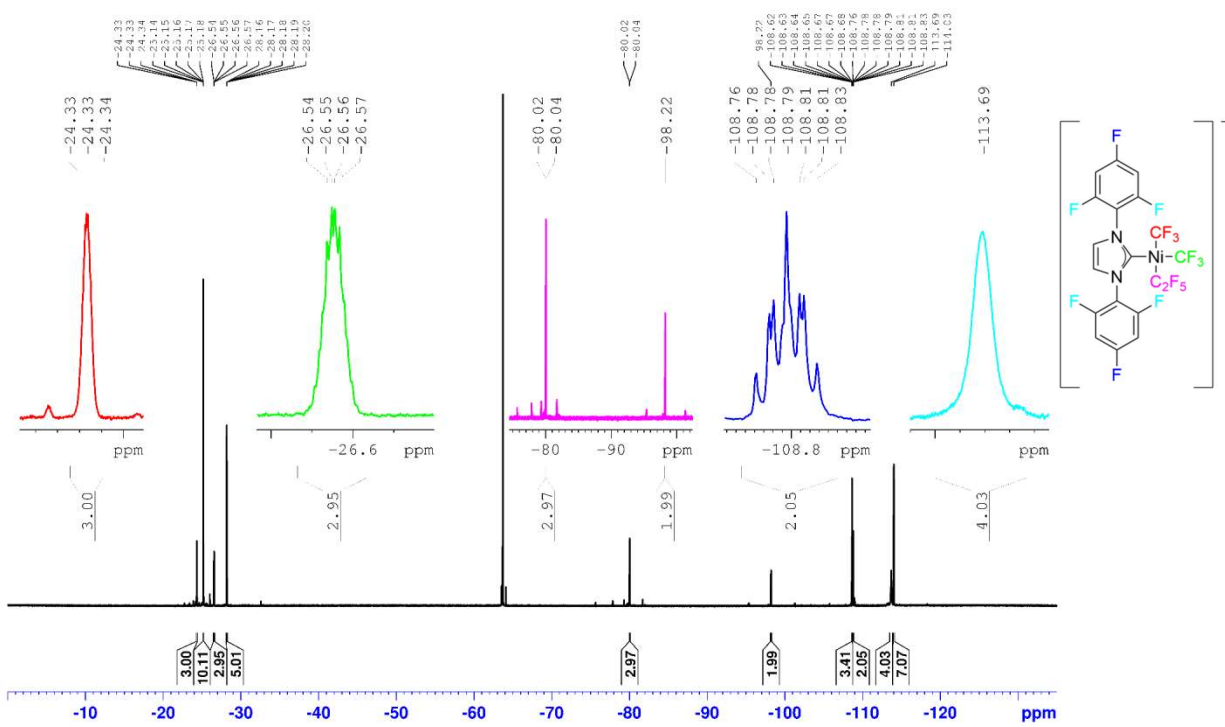
Fig. S22C 400 MHz ^{1}H NMR and 470.6 MHz ^{19}F NMR spectra of **8** and **8′** in CD$_3$CN.
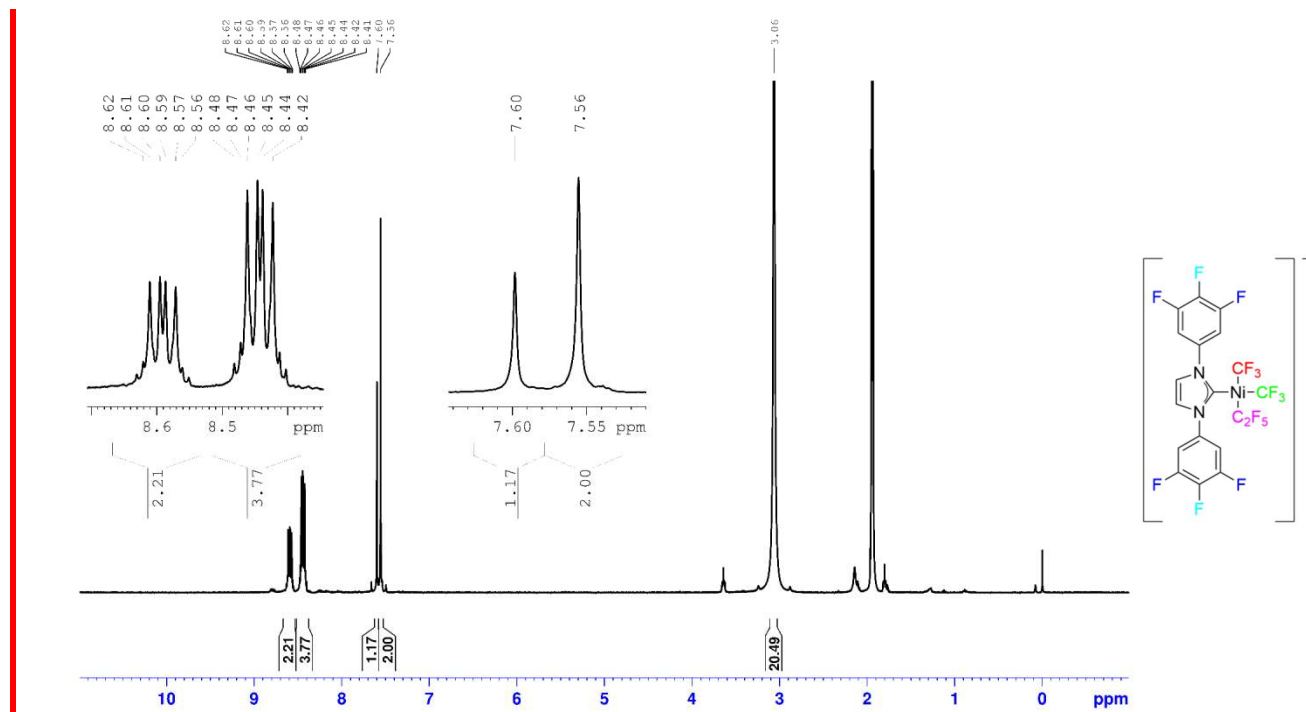
Fig. S23A 400 MHz ^{1}H NMR and 470.6 MHz ^{19}F NMR spectra of **9** and **9′** in CD$_3$CN.
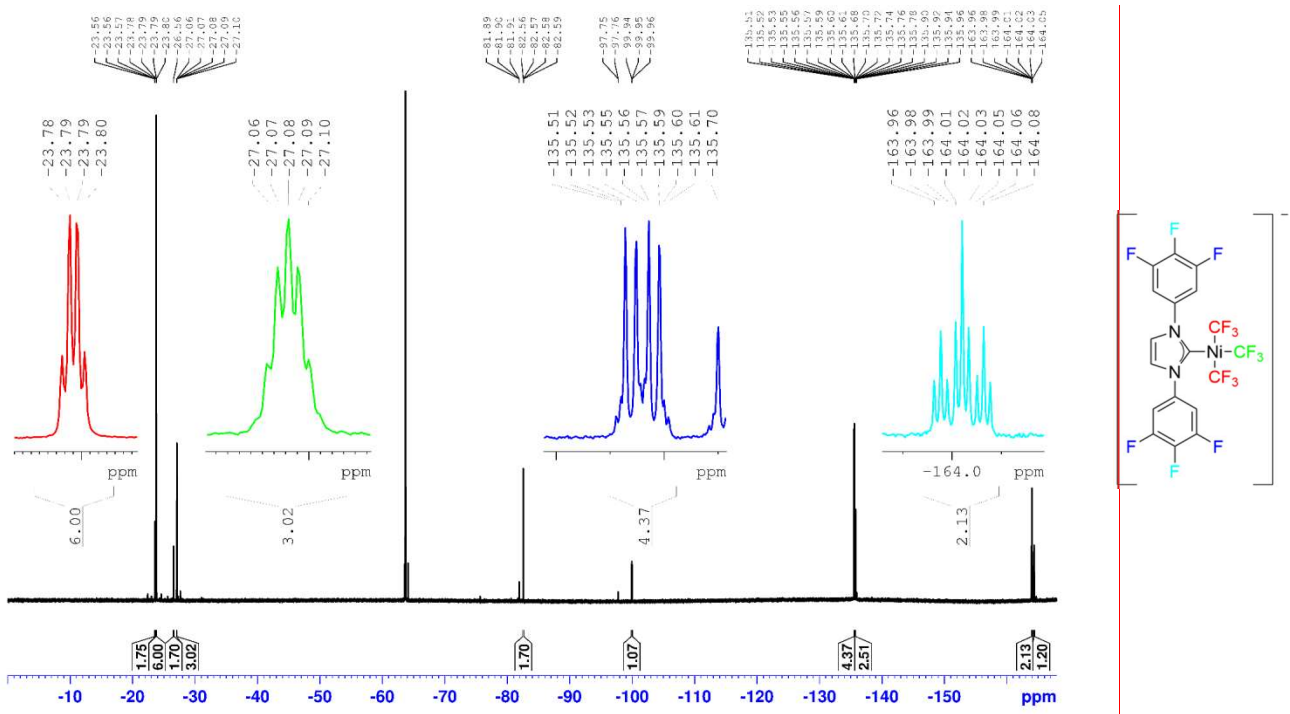
**Fig. S23B** 400 MHz ¹H NMR and 470.6 MHz ¹⁹F NMR spectra of **9** and **9′** in CD₃CN.
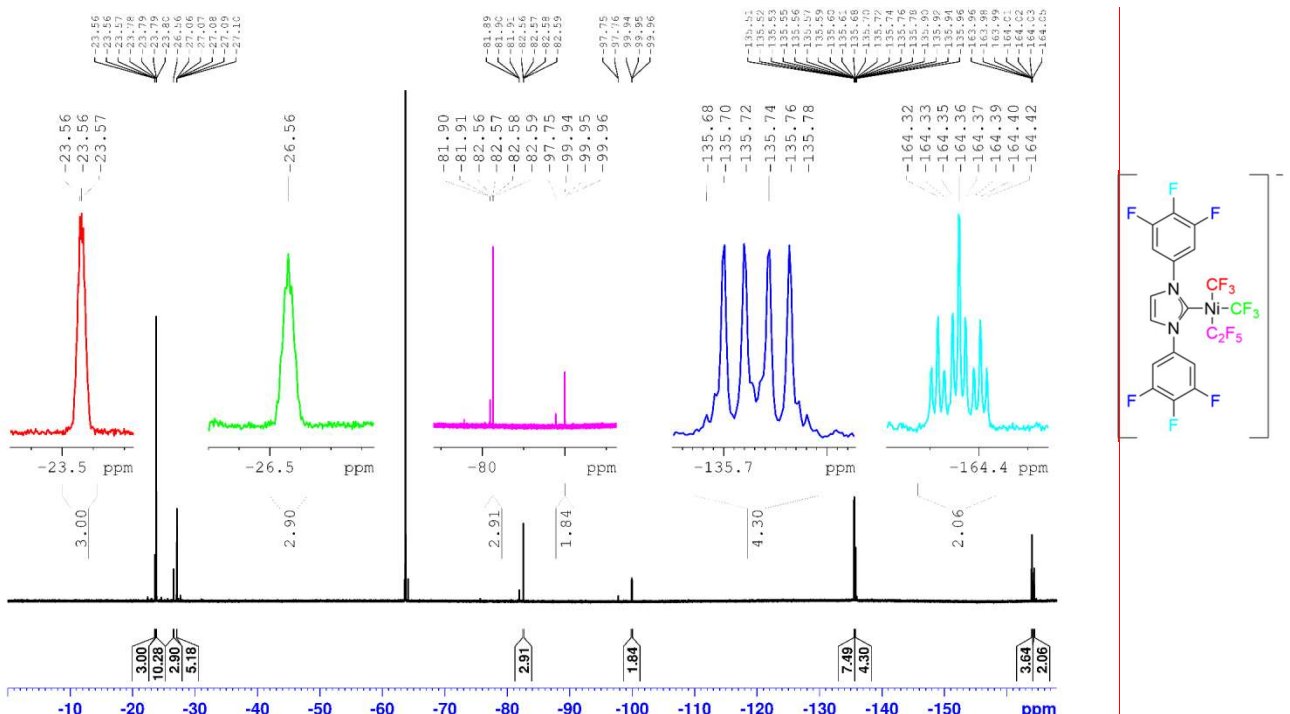
Fig. S23C 400 MHz ¹H NMR and 470.6 MHz ¹⁹F NMR spectra of **9** and **9′** in CD₃CN.
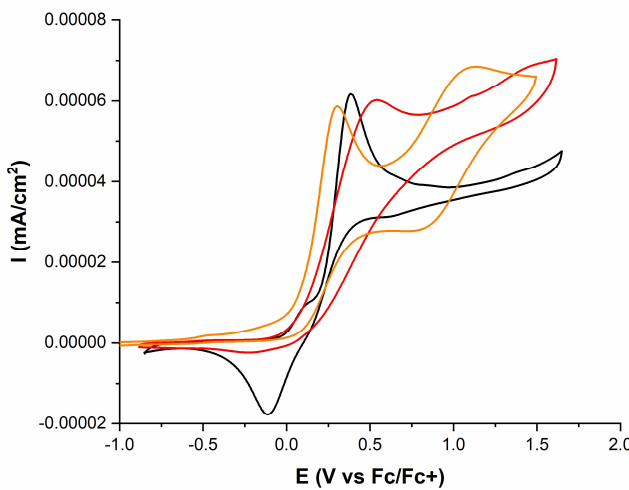
Fig. S24 Cyclic voltammograms of **1** (black), **2** (red), and **4** (orange) in MeCN/n-Bu$_4$NPF$_6$.
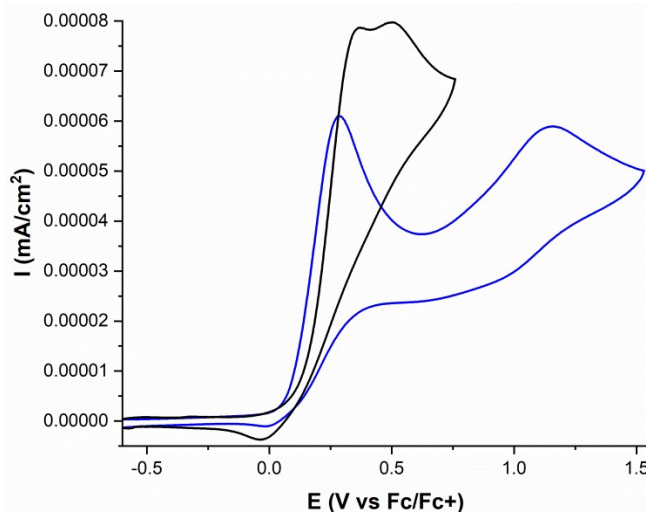
Fig. S25 Cyclic voltammograms of **5** (black) and **6** (blue) in MeCN/n-Bu$_4$NPF$_6$.
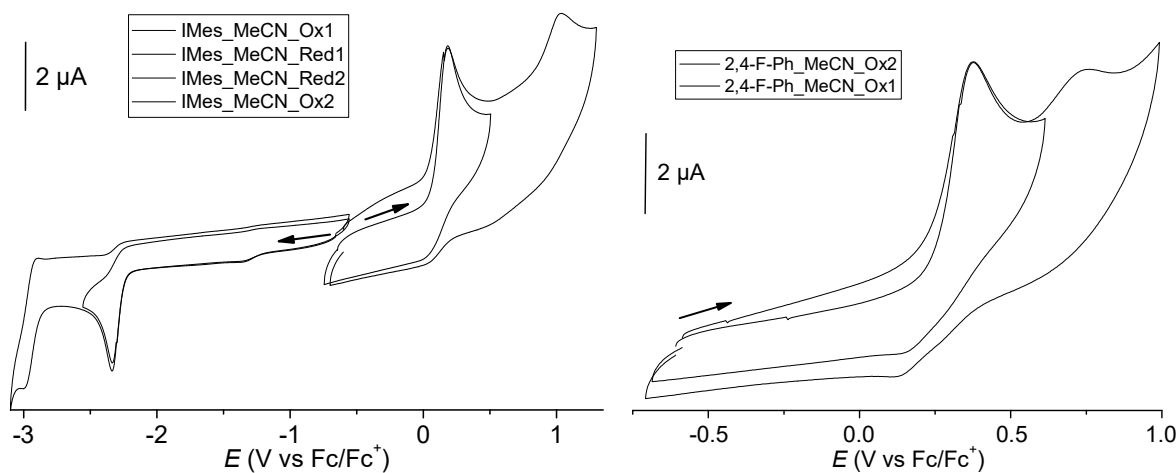
Fig. S26 Cyclic voltammograms of [NEt$_4$][(IMes)Ni(CF$_3$)$_3$] (**6**) (left) and [NEt$_4$][(2,4-F$_2$Ph-NHC)Ni(CF$_3$)$_3$] (**7**) (right) in MeCN/n-Bu$_4$NPF$_6$.
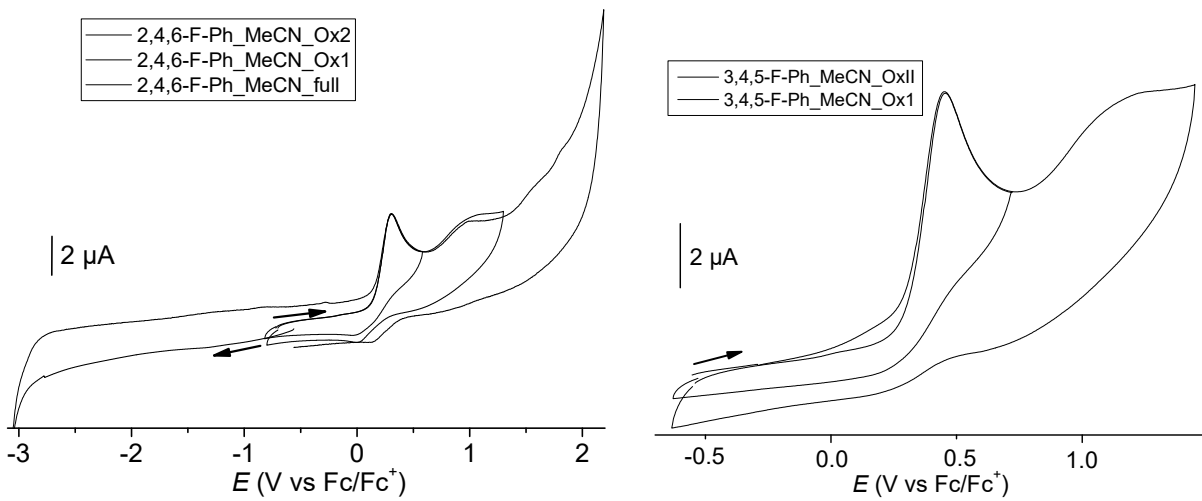
Fig. S27 Cyclic voltammograms of [NEt₄][(2,4,6-F₃Ph-NHC)Ni(CF₃)₃] (**8**) (left) and [NEt₄][(3,4,5-F₃Ph-NHC)Ni(CF₃)₃] (**9**) (right) in MeCN/n-Bu₄NPF₆.

Table S1. Selected structure solution and refinement data for nickel complexes

| compound	[PPh₄][(IMes)Ni(CF₃)₃] (**6′**)	[NMe₄][(2,4-F₂Ph-NHC)Ni(CF₃)₃] (**7**)	[NMe₄][(3,4,5-F₃Ph-NHC)Ni(CF₃)₃] (**9**)	[NMe₄][(3,4,5-F₃Ph-NHC)Ni(CF₃)₂(C₂F₅)](**9′**)
Formula	C₅₀H₄₇F₉N₃NiP	C₂₂.₁₄H₂₀F₁₃.₀₃N₃Ni	C₂₂H₁₈F₁₅N₃Ni	C₃₁.₂H₃₃.₃₁F₁₆.₉₂N₃NiO₂
F.W. (g/mol)	950.58	634.48	668.10	862.57
T (K)	100.0	293(2)	100.0	100.0
crystal system	Monoclinic	Triclinic	Monoclinic	Triclinic
space group	$C2/c$	$P{-}1$	$P2_1/c$	$P{-}1$
cell a (Å)	19.9610(11)	9.9583(3)	15.9285(11)	8.5261(3)
b (Å)	11.2347(6)	10.3755(5)	9.6940(6)	13.2144(5)
c (Å)	40.329(2)	12.8434(6)	16.2880(9)	16.9930(6)
α (°)	90	69.438(4)	90	104.8370(10)
β (°)	97.043(2)	87.104(3)	95.067(2)	91.5500(10)
γ (°)	90	82.992(3)	90	105.7390(10)
Volume (Å³)	8975.8(9)	1233.15(10)	2505.2(3)	1771.72(11)
Z	8	2	4	2
dens. calc. (g/cm³)	1.407	1.709	1.771	1.617
ab. coeff. (cm⁻¹)	5.42	3.52	9.05	6.71
$F(000)$	3936.0	638.0	1336.0	876.0
θ range (°)	4.07 to 59.198	2.968 to 63.002	4.894 to 52.836	4.674 to 52.77
Index ranges	−27 ≤ h ≤ 27, −15 ≤ k ≤ 15, −56 ≤ l ≤ 55	−17 ≤ h ≤ 17, −20 ≤ k ≤ 20, −26 ≤ l ≤ 26	−19 ≤ h ≤ 19, −12 ≤ k ≤ 12, −20 ≤ l ≤ 20	−10 ≤ h ≤ 10, −16 ≤ k ≤ 16, −21 ≤ l ≤ 21
Refl. coll.	137625	27658	42484	78752
Indep. refl.	12599	15287	5140	7250
Comp. to θ	0.999	0.648	0.998	0.999
Data/rest./param.	12599/24/621	15287/73/461	5140/0/402	7250/207/640
G-o-f on F^2	0.984	0.805	1.044	1.031
Final R indices	R₁ = 0.0490, wR₂ =	R₁ = 0.0577, wR₂ =	R₁ = 0.0665, wR₂ =	R₁ = 0.0439, wR₂ = 0.1177

[I>2sigma(I)]	0.1038	0.1497	0.1861	
R indices (all data)	R_1 = 0.0596, wR_2 = 0.1091	R_1 = 0.1216, wR_2 = 0.1617	R_1 = 0.0831, wR_2 = 0.2004	R_1 = 0.0498, wR_2 = 0.1223
Ext. coeff.	None	0.009832	0.1109	None
Largest diff. peak and hole	0.49/–0.43	1.48/–0.83	1.64/–0.71	0.97/–0.55
CCDC	2095551	2103215	2118416	2126925

Table S2 Selected structure solution and refinement data for $[PNP]_2[Ni_2(CF_3)_4(\mu\text{-}F)_2]\cdot 2THF$.

compound	$[PNP]_2[Ni_2(CF_3)_4(\mu\text{-}F)_2]\cdot 2THF$
Formula	$C_{84}H_{76}F_{14}N_2Ni_2O_2P_4$
formula weigth (g/mol)	1652.76
T (K)	120.0
crystal system	Monoclinic
space group	$P2_1/c$
cell a (Å)	11.807(2)
b (Å)	20.672(4)
c (Å)	15.556(3)
α (°)	90
β (°)	94.953(7)
γ (°)	90
Volume (Å³)	3782.6(11)
Z	2
density calculated (g/cm³)	1.451
absorption coefficient (cm⁻¹)	6.67
$F(000)$	1704.0
Theta range for data collection (°)	3.94 to 52.836
Index ranges	$-14 \le h \le 14$, $-25 \le k \le 25$, $-18 \le l \le 19$
Reflections collected	83345
Independent reflections	7749
Completeness to theta	0.997
Data / restraints / parameters	7749/0/487
Goodness-of-fit on F^2	1.041
Final R indices [I>2sigma(I)]	R_1 = 0.0401, wR_2 = 0.0979
R indices (all data)	R_1 = 0.0530, wR_2 = 0.1056
Extinction coefficient	0.0511
Largest diff. peak and hole	0.69/–0.52
CCDC	2126925